

# Mechanisms of Altered Excitation-Contraction Coupling in Canine Tachycardia-Induced Heart Failure, I

## Experimental Studies

Brian O'Rourke, David A. Kass, Gordon F. Tomaselli, Stefan Kääb, Richard Tunin, Eduardo Marbán

**Abstract**—Pacing-induced heart failure in the dog recapitulates many of the electrophysiological and hemodynamic abnormalities of the human disease; however, the mechanisms underlying altered  $\text{Ca}^{2+}$  handling have not been investigated in this model. We now show that left ventricular midmyocardial myocytes isolated from dogs subjected to 3 to 4 weeks of rapid pacing have prolonged action potentials and  $\text{Ca}^{2+}$  transients with reduced peaks, but durations  $\approx 3$ -fold longer than controls. To discriminate between action potential effects on  $\text{Ca}^{2+}$  kinetics and direct changes in  $\text{Ca}^{2+}$  regulatory processes, voltage-clamp steps were used to examine the time constant for cytosolic  $\text{Ca}^{2+}$  removal ( $\tau_{\text{Ca}}$ ).  $\tau_{\text{Ca}}$  was prolonged by just 35% in myocytes from failing hearts after fixed voltage steps in physiological solutions ( $\tau_{\text{Ca}}$  control,  $216 \pm 25$  ms,  $n=17$ ;  $\tau_{\text{Ca}}$  failing,  $292 \pm 23$  ms,  $n=22$ ;  $P < 0.05$ ), but this difference was markedly accentuated when  $\text{Na}^+/\text{Ca}^{2+}$  exchange was eliminated ( $\tau_{\text{Ca}}$  control,  $282 \pm 30$  ms,  $n=13$ ;  $\tau_{\text{Ca}}$  failing,  $576 \pm 83$  ms,  $n=11$ ;  $P < 0.005$ ). Impaired sarcoplasmic reticular (SR)  $\text{Ca}^{2+}$  uptake and a greater dependence on  $\text{Na}^+/\text{Ca}^{2+}$  exchange for cytosolic  $\text{Ca}^{2+}$  removal was confirmed by inhibiting SR  $\text{Ca}^{2+}$  ATPase with cyclopiazonic acid, which slowed  $\text{Ca}^{2+}$  removal more in control than in failing myocytes.  $\beta$ -Adrenergic stimulation of SR  $\text{Ca}^{2+}$  uptake in cells from failing hearts sufficed only to accelerate  $\tau_{\text{Ca}}$  to the range of unstimulated controls. Protein levels of SERCA2a, phospholamban, and  $\text{Na}^+/\text{Ca}^{2+}$  exchanger revealed a pattern of changes qualitatively similar to the functional measurements; SERCA2a and phospholamban were both reduced in failing hearts by 28%, and  $\text{Na}^+/\text{Ca}^{2+}$  exchange protein was increased 104% relative to controls. Thus, SR  $\text{Ca}^{2+}$  uptake is markedly downregulated in failing hearts, but this defect is partially compensated by enhanced  $\text{Na}^+/\text{Ca}^{2+}$  exchange. The alterations are similar to those reported in human heart failure, which reinforces the utility of the pacing-induced dog model as a surrogate for the human disease. (*Circ Res.* 1999;84:562-570.)

**Key Words:** excitation-contraction coupling ■ action potential ■ sarcoplasmic reticulum ■  $\text{Ca}^{2+}$  uptake ■ heart failure

Recent evidence indicates that the hemodynamic alterations accompanying heart failure are coincident with a common pattern of electrophysiological and excitation-contraction (E-C) coupling changes at the cellular level. Hallmarks of heart failure include prolongation of the cardiac action potential,<sup>1-4</sup> downregulation of the repolarizing potassium currents  $I_{\text{to}}$  and  $I_{\text{K1}}$ ,<sup>1,5,6</sup> decreased responsiveness to  $\beta$ -adrenergic stimulation,<sup>7-13</sup> and alterations of intracellular  $\text{Ca}^{2+}$  handling.<sup>14-17</sup> Studies of intact cardiac muscles<sup>18-20</sup> or isolated myocytes<sup>21,22</sup> indicate that developed force is depressed, relaxation is prolonged, and frequency-dependent facilitation of contraction is blunted in heart failure. These findings may be explained by underlying defects in cellular  $\text{Ca}^{2+}$  homeostasis. The amplitude of the intracellular  $\text{Ca}^{2+}$  transient and its rate of decay have been shown to be reduced in intact muscles<sup>15</sup> and in isolated ventricular myocytes<sup>2,23,24</sup> from failing human hearts.

Although there is strong evidence that intracellular  $\text{Ca}^{2+}$  removal is suppressed in heart failure, there is still contro-

versy about which  $\text{Ca}^{2+}$  regulatory proteins are responsible for the changes in  $\text{Ca}^{2+}$  homeostasis. Numerous investigators have reported that the levels of sarcoplasmic reticular (SR)  $\text{Ca}^{2+}$  ATPase (SERCA2) mRNA are reduced by  $\approx 50\%$  in human heart failure (reviewed in References 25 and 26), and Hasenfuss et al<sup>18</sup> reported a 30% to 40% reduction of SERCA2 protein levels by Western blot associated with a reduction in SR  $^{45}\text{Ca}$  uptake. The latter result contrasts with several reports that have shown no change in pump protein level,<sup>27-29</sup> either with<sup>29</sup> or without<sup>30</sup> a concomitant change in function. Similar disparate results have been reported for the  $\text{Ca}^{2+}$  ATPase regulatory protein phospholamban (PLB), ie, reduced message levels, but there is disagreement about whether PLB protein expression is decreased.  $\text{Na}^+/\text{Ca}^{2+}$  exchange, the other major  $\text{Ca}^{2+}$  removal system of the heart, is apparently upregulated in the failing heart. mRNA levels of the exchanger were shown to be increased 55% to 79%<sup>31,32</sup> in human dilated cardiomyopathy, while the amount of  $\text{Na}^+$

Received April 27, 1998; accepted December 18, 1998.

From the Section of Molecular and Cellular Cardiology, Division of Cardiology, Department of Medicine, The Johns Hopkins University, Baltimore, Md.

This manuscript was sent to Harry A. Fozzard, Consulting Editor, for review by expert referees, editorial decision, and final disposition.

Correspondence to Brian O'Rourke, PhD, Division of Cardiology, Department of Medicine, The Johns Hopkins University, 844 Ross Building, 720 Rutland Avenue, Baltimore, MD 21205. E-mail bor@jhmi.edu

© 1999 American Heart Association, Inc.

Circulation Research is available at <http://www.circresaha.org>

$\text{Ca}^{2+}$  exchange protein was increased 36% to 160% in several studies.<sup>31–34</sup> It has been suggested that the reduction in SR function, coupled with compensatory upregulation of  $\text{Na}^+/\text{Ca}^{2+}$  exchange, may underlie the blunted force-frequency relation and postrest potentiation evident in heart failure, but it may also serve as a positive inotropic mechanism under  $\text{Na}^+$ -loaded conditions.<sup>32</sup>

The present study examines in detail the E-C coupling alterations in the canine ventricular tachycardia-induced heart failure model to investigate the mechanism underlying the prolongation of  $\text{Ca}^{2+}$  removal. In addition, the profile of altered  $\text{Ca}^{2+}$  regulatory proteins was assessed by Western blot analysis. The finding that the burden of  $\text{Ca}^{2+}$  removal is shifted from SR  $\text{Ca}^{2+}$  uptake to  $\text{Ca}^{2+}$  extrusion via  $\text{Na}^+/\text{Ca}^{2+}$  exchange is similar to what is thought to occur in human heart failure, supporting the notion that a fundamental program of ionic and E-C coupling alterations is induced by heart failure. The contribution of these changes to the shape and duration of the cardiac action potential and intracellular  $\text{Ca}^{2+}$  transient are tested by incorporating the experimental results into a computer model of the canine cardiomyocyte, as described in the accompanying study.<sup>35</sup>

## Materials and Methods

### Pacing-Induced Failure Protocol and Isolation of Midmyocardial Cardiomyocytes

Induction of heart failure and ventricular cardiomyocyte isolation were carried out as described previously<sup>1</sup> using protocols approved by the institution's Animal Care and Use Committee. In brief, mongrel dogs of either sex were anesthetized and surgically instrumented under sterile conditions for implantation of a VVI pacemaker (Medtronic). Rapid pacing at 240 bpm was initiated 1 to 2 days after surgery and maintained for 3 to 4 weeks. At terminal heart failure (verified by hemodynamic measurements),<sup>1</sup> hearts were harvested by left lateral thoracotomy, immersed in ice-cold saline, and quickly excised. Control hearts were similarly obtained from nonpaced dogs. The region of the ventricle perfused by the left anterior descending coronary artery was excised, cannulated, and perfused at 15 mL/min with nominally  $\text{Ca}^{2+}$ -free modified Tyrode's solution (in mmol/L, NaCl 138, KCl 4,  $\text{MgCl}_2$  1,  $\text{NaH}_2\text{PO}_4$  0.33, glucose 10, and HEPES 10 [pH 7.3 with NaOH] at 37°C and oxygenated with 100%  $\text{O}_2$ ) for 30 minutes; with the same solution with added collagenase (type I, 178 U/mL, Worthington Biochemical Corp) and protease (type XIV, 0.12 mg/mL, Sigma) for 40 minutes; and with washout solution (with 200  $\mu\text{mol/L}$   $\text{CaCl}_2$ ) for 15 minutes. Chunks of well-digested ventricular tissue from the midmyocardial layer of the ventricle were dissected out, and myocardial cells were mechanically disaggregated, filtered through nylon mesh, and stored in modified Tyrode's solution containing 2 mmol/L  $\text{Ca}^{2+}$ . The procedure yielded  $\text{Ca}^{2+}$ -tolerant quiescent myocytes with clear striations and no visible abnormalities (such as granules, blebs, etc).

### Single-Cell Physiological Studies

Isolated ventricular myocytes were placed in a heated (37°C) chamber on the stage of an inverted fluorescence microscope (Diaphot 200; Nikon, Inc) and superfused with a physiological salt solution containing (in mmol/L) NaCl 138, KCl 4,  $\text{MgCl}_2$  1,  $\text{CaCl}_2$  2,  $\text{NaH}_2\text{PO}_4$  0.33, glucose 10, and HEPES 10 (pH 7.4 with NaOH) or with an  $\text{Na}^+$ -free solution for measurement of  $\text{Ca}^{2+}$  transient decay in the absence of  $\text{Na}^+/\text{Ca}^{2+}$  exchange containing (in mmol/L) *N*-methyl  $\text{D}$ -glucamine 140,  $\text{MgCl}_2$  0.5,  $\text{CaCl}_2$  2, CsCl 4, glucose 10, and HEPES 10 (pH 7.4 with HCl). Intracellular solutions contained either a physiological ionic composition consisting of (in mmol/L) potassium glutamate 130, KCl 9, NaCl 10,  $\text{MgCl}_2$  0.5, and MgATP 5, and HEPES 10 (pH 7.2 with KOH) and 80  $\mu\text{mol/L}$  indo-1 (Molecular Probes) or an  $\text{Na}^+$ -free internal solution containing (in mmol/L)

glutamate 130, CsCl 20,  $\text{MgCl}_2$  0.5, MgATP 5, and HEPES 10 (pH 7.2 with CsOH) and 80  $\mu\text{mol/L}$  indo-1.

Borosilicate glass pipets of 1- to 4-M $\Omega$  tip resistance were used for whole-cell recording of action potentials or membrane currents with an Axopatch 200A amplifier coupled to a Digidata 1200A personal computer interface (Axon Instruments). A xenon arc lamp was used to excite indo-1 fluorescence at 365 nm (390 nm dichroic mirror), and the emitted fluorescence was recorded using a dual channel photomultiplier tube assembly (ESP associates, Toronto, Ontario) at wavelengths of 405 and 495 nm. Cellular autofluorescence at both emission wavelengths was recorded before rupturing the cell-attached patch. Electrophysiological and fluorescence signals were acquired simultaneously and analyzed offline with custom-written software (IonView, B. O'Rourke).

On establishing the whole-cell configuration, 10-mV depolarizing test pulses from a holding potential of  $-80$  mV were applied to examine the passive membrane properties of the myocytes. Cell capacitance ( $C_m$ ), determined by integrating the area under the capacitive current trace (control,  $152 \pm 8$  pF,  $n=59$ ; failing,  $175 \pm 8$  pF;  $n=28$ ), and series resistance (control,  $7.8 \pm 1.0$  M $\Omega$ ,  $n=59$ ; failing,  $6.1 \pm 0.6$  M $\Omega$ ,  $n=28$ ), determined from the exponential time constant of current decay ( $R_s = C_m/\tau_m$ ), did not differ between groups. Membrane capacitance and series resistance were electrically compensated by 70 to 75% for an estimated maximal voltage error of  $<3$  mV in voltage-clamp mode. Compensation was disabled in current-clamp mode. Data have been corrected post hoc for the measured liquid junction potentials between the pipet and bath solutions as described.<sup>36</sup>

The ratio of indo-1 fluorescence ( $R = F_{405 \text{ nm}}/F_{495 \text{ nm}}$ ) was determined after subtraction of cellular autofluorescence and was used to calculate free intracellular  $\text{Ca}^{2+}$  according to the equation  $[\text{Ca}^{2+}]_i = K_d \times \beta [(R - R_{\text{min}})/(R_{\text{max}} - R)]$ ,<sup>37</sup> using a  $K_d$  of 844 nmol/L, as reported for rabbit cardiomyocytes.<sup>38</sup> The average  $R_{\text{min}}$ ,  $R_{\text{max}}$ , and  $\beta$  for the fluorescence system were determined by sequential exposure of cardiomyocytes to (1) a zero- $\text{Ca}^{2+}$  modified Tyrode's solution (other components as described above) containing metabolic inhibitors (10 mmol/L 2-deoxyglucose and 100  $\mu\text{mol/L}$  2,4-dinitrophenol), (2) the same solution with 1 mmol/L EGTA and 20  $\mu\text{mol/L}$  ionomycin (for  $R_{\text{min}}$ ), and (3) and a high  $\text{Ca}^{2+}$  Tyrode's solution (5 mmol/L  $\text{Ca}^{2+}$  instead of EGTA) for determining  $R_{\text{max}}$ .  $R_{\text{min}}$ ,  $R_{\text{max}}$ , and  $\beta$  were  $1.24 \pm 0.09$ ,  $10.44 \pm 1.85$ , and  $2.7 \pm 0.4$ , respectively ( $n=10$ ).

The duration of action potential-stimulated  $\text{Ca}^{2+}$  transients was determined by measuring the time from electrical stimulation to the half-decay of the transient from its peak ( $\text{CaD}_{50}$ ). The time constant for  $\text{Ca}^{2+}$  removal ( $\tau_{\text{Ca}}$ ) was determined by fitting a single exponential to the  $\text{Ca}^{2+}$  transient during the late phase of repolarization of the action potential or, for voltage clamp pulses,  $\approx 20$  ms after returning to the holding potential after a stimulus. Peak systolic  $\text{Ca}^{2+}$  was measured at steady state for a given stimulation frequency, which usually occurred after 10 to 15 pulses to a single test potential.

### Western Blot Analysis

Chunks of left ventricle from the same hearts used for physiological study were freeze-clamped in liquid nitrogen at the time of sacrifice and stored at  $-80^\circ\text{C}$ . Frozen tissue samples were pulverized with a mortar and pestle, and 10 mL/g of wet tissue weight of lysis buffer was added (pH 7.0) (buffer contained [in mmol/L] NaCl 145,  $\text{MgCl}_2$  0.1, HEPES 15, EGTA 10, and Triton X-100 0.5 and protease inhibitors [in  $\mu\text{mol/L}$ , aminoethyl benzenesulfonyl fluoride 500, aprotinin 0.2, antipain 1.7, leupeptin 1, and chymostatin 10]). After a 30-minute incubation period on ice, the lysate was homogenized (two 15-second bursts) and centrifuged, and the supernatant was aliquoted into tubes and frozen for subsequent analysis. The protein concentration was assayed (BCA kit, Pierce Biochemicals), and 100  $\mu\text{L}$  of lysate was added to an equal volume of sample buffer containing 50 mmol/L Tris-HCl, 10% glycerol, 2% SDS, 0.05% bromophenol blue, and 0.3 mmol/L DTT and boiled for 5 minutes. Triplicate samples from 1 control heart and 1 failing heart were loaded on each 5% to 15% polyacrylamide gradient gel (Ready Gel, Bio-Rad) along with duplicate samples from a control heart selected as a reference for data normalization. After electrophoretic separation at 200 V for 30 to 45 minutes in Tris-glycine/SDS buffer

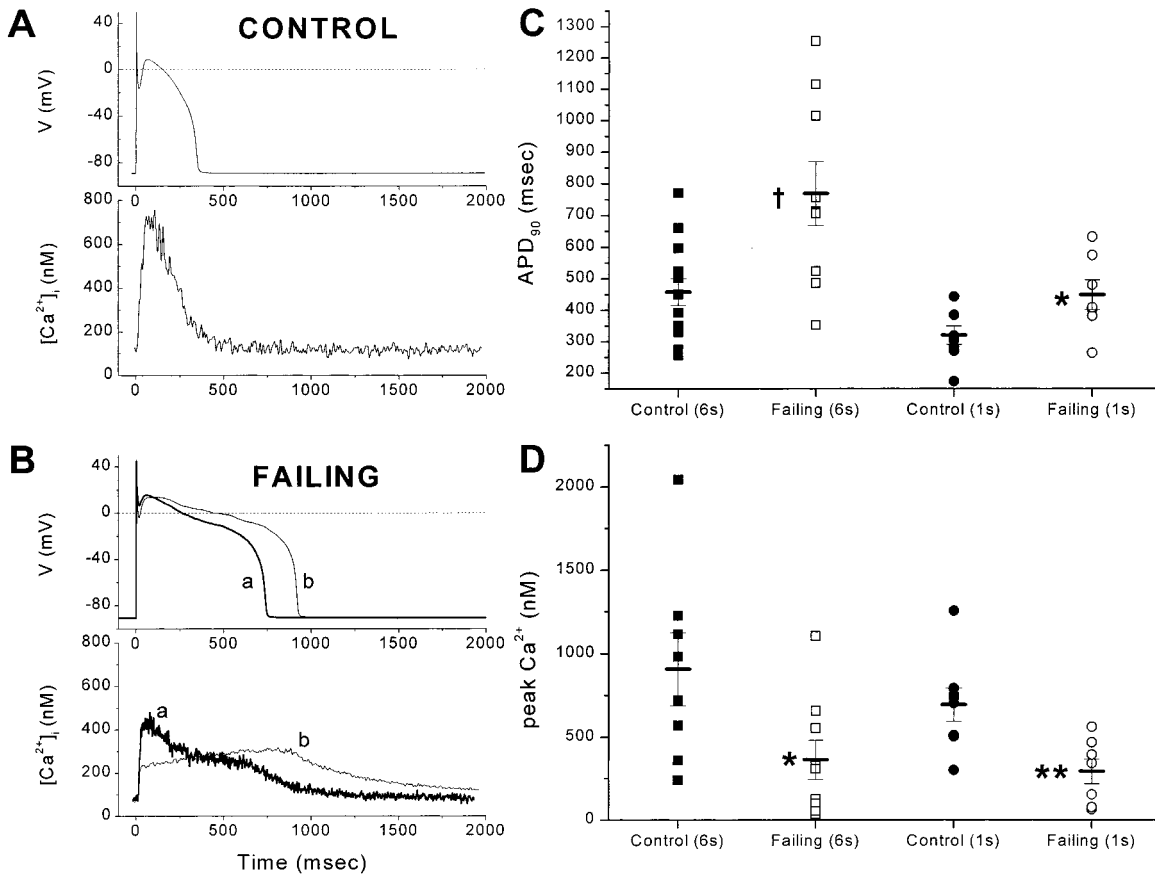


**Figure 1.** Action potentials and cytosolic Ca<sup>2+</sup> transients in cardiomyocytes from control and failing canine hearts. A, An action potential (top panel) and its associated Ca<sup>2+</sup> transient (bottom panel) in a myocyte from a control heart in physiological solution (cycle length, 6 seconds). B, Prolonged action potentials (top panel) and Ca<sup>2+</sup> transients (bottom panel) in a myocyte from a failing heart. Examples of moderately (a) and severely (b) impaired SR Ca<sup>2+</sup> release are shown, as described in the text (cycle length, 6 seconds). C and D, Distribution of APD<sub>90</sub> (C) and peak systolic Ca<sup>2+</sup> amplitudes (D), and their averages, for myocytes from control and failing hearts at 6- or 1-second cycle lengths. ■, □, ●, and ○ represent values of individual myocytes from 5 control hearts and 5 failing hearts; horizontal bars represent mean ± SE for each data set. \*\**P* < 0.005, \**P* < 0.05, †*P* < 0.01 for comparisons between control and failing groups.

(Mini Protean II apparatus, Bio-Rad) proteins were transferred to nitrocellulose membranes (Semi-Dry transfer blot, Bio-Rad), and non-specific antibody binding was blocked for 1 hour in PBS with 0.1% Tween-20 and 5% nonfat milk. Membranes were washed for 15 minutes in Tween/PBS and then incubated with the primary antibody of interest for 1 hour. Monoclonal anti-SERCA2 (catalog No. MA3-919), anti-PLB (catalog No. MA3-922) and anti-Na<sup>+</sup>/Ca<sup>2+</sup> exchanger (NCX) (catalog No. MA3-926) antibodies were purchased from Affinity BioReagents (Golden, CO). After washout of the primary antibody, membranes were incubated for 1 hour with anti-immunoglobulin horseradish peroxidase secondary antibody and extensively washed again before chemiluminescent detection on Hyperfilm enhanced chemiluminescence (Amersham Life Science, Inc).

Films were digitally scanned into a computer, and band densities were corrected for protein loading (which was approximately equal for all samples on a gel) and normalized to the average density of the reference lanes for comparison of control and failing heart samples. Band density was linearly related to protein loading (data not shown).

### Statistical Analysis

Comparisons between groups were made using unpaired Student *t* tests or, for data spanning a range of conditions (eg, frequency dependence of action potential duration [APD]), by 2-factor ANOVA followed by the Tukey test. ANCOVA was used to examine the relation between the Ca<sup>2+</sup> transient duration and APD. A 95% CI was used to determine statistical significance.

## Results

### Action Potential–Stimulated Ca<sup>2+</sup> Transients

Action potentials recorded at 37°C with minimal intracellular Ca<sup>2+</sup> buffering (80 μmol/L indo-1) were prolonged in myocytes from failing hearts (Figure 1B) relative to those from control hearts (Figure 1A; 6-second cycle length). The morphology of the accompanying Ca<sup>2+</sup> transients (Figure 1A and 1B, bottom panels) also differed, with the majority of transients in cells from failing hearts displaying a biphasic time to peak consisting of a fast peak at 43 ± 7 ms (n = 9) after stimulus and a slowly rising phase, which depended on the duration of depolarization. In Figure 1B, 2 examples of representative action potentials and Ca<sup>2+</sup> transients are superimposed to illustrate the differential extent of SR impairment among cells from failing hearts. The large early peak in the transient, which is suppressed by ryanodine or cyclopiazonic acid (CPA; compare with Figure 5), represents Ca<sup>2+</sup> release from the SR (compare with Figure 3 of Winslow et al.<sup>35</sup> In contrast, the typical control myocyte had a Ca<sup>2+</sup> transient with a rapid time to peak (32 ± 3 ms, n = 10; NS with respect to the failing group) and the onset of Ca<sup>2+</sup> decay preceding repolarization. Despite a substantial amount of overlap of the data ranges between groups (as evidenced by the scatter plots in

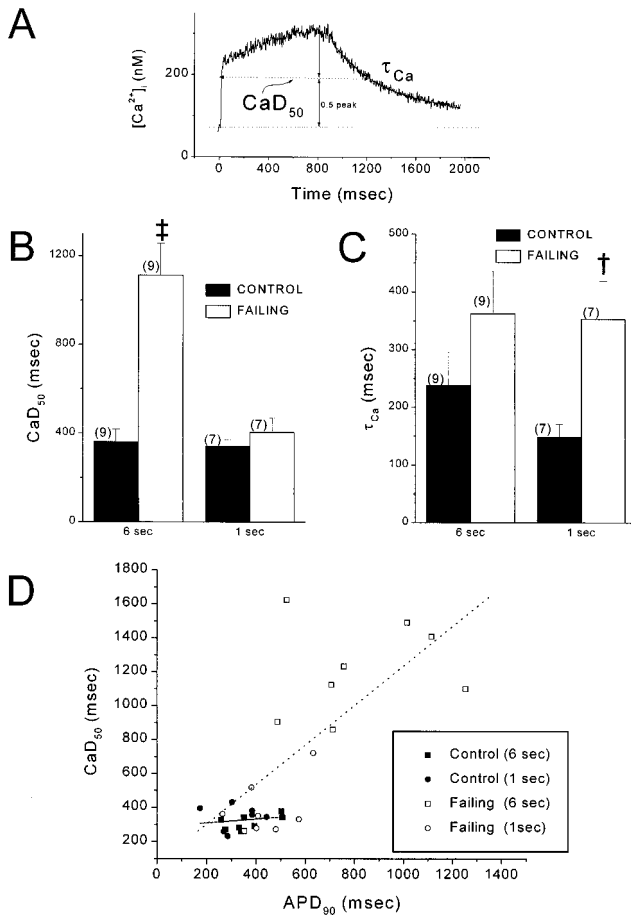


**Figure 2.** Parameters of  $\text{Ca}^{2+}$  decline in myocytes from control and failing hearts. A, Determination of the time from stimulus to  $\text{CaD}_{50}$  was made by measuring the time at which  $\text{Ca}^{2+}$  crossed the half-amplitude (50% of the difference between peak and diastolic  $\text{Ca}^{2+}$ ) point of the  $\text{Ca}^{2+}$  record. The exponential time constant for  $\text{Ca}^{2+}$  decay ( $\tau_{\text{Ca}}$ ) was fit during the late phase of the action potential. B and C,  $\text{CaD}_{50}$  and  $\tau_{\text{Ca}}$  at 6- and 1-second cycle lengths. Data are mean  $\pm$  SE.  $\dagger P < 0.01$ ;  $\ddagger P < 0.001$ . D, Correlation between  $\text{CaD}_{50}$  and the APD ( $\text{APD}_{90}$ ), with lines indicating fits of data from control (dashed line) and failing (dotted line) hearts.

Figure 1C), statistically significant differences in APD with heart failure were evident at both 6- and 1-second cycle lengths (Figure 1C). The amplitude of the  $\text{Ca}^{2+}$  transient also differed between groups: peak systolic  $\text{Ca}^{2+}$  was significantly higher in control myocytes at both the 6-second (control,  $908 \pm 218$  nmol/L,  $n=8$ ; failing,  $363 \pm 125$  nmol/L,  $n=9$ ;  $P < 0.05$ ) and the 1-second (control,  $695 \pm 106$  nmol/L,  $n=8$ ; failing,  $294 \pm 81$  nmol/L,  $n=7$ ;  $P < 0.01$ ) stimulus intervals. Although diastolic  $\text{Ca}^{2+}$  tended to be lower in myocytes from failing hearts, this difference was not significant (control, 6 seconds,  $153 \pm 22$  nmol/L,  $n=9$ ; failing, 6 seconds,  $64 \pm 42$  nmol/L,  $n=9$ ; control, 1 second,  $187 \pm 22$  nmol/L,  $n=8$ ; failing, 1 second,  $64 \pm 42$  nmol/L,  $n=7$ ).

The duration of the  $\text{Ca}^{2+}$  transients, as measured from the stimulus to  $\text{CaD}_{50}$  (illustrated in Figure 2A) was 3-fold longer in myocytes from failing hearts at the 6-second stimulus interval (Figure 2B; control,  $362 \pm 55$  ms,  $n=9$ ; failing,  $1112 \pm 145$  ms,  $n=9$ ;  $P < 0.001$ ). This difference was substantially less at the 1-second cycle length (Figure 2B; control,  $342 \pm 30$  ms,  $n=7$ ; failing,  $404 \pm 66$  ms,  $n=7$ ; NS), paralleling

the effect of frequency on the APD (compare Figure 1C with Figure 2B). The latter finding suggested that the duration of the  $\text{Ca}^{2+}$  transient was strongly influenced by membrane potential in myocytes from failing hearts. This was supported by correlating  $\text{CaD}_{50}$  with APDs at 90% repolarization ( $\text{APD}_{90}$ ) (Figure 2D).  $\text{CaD}_{50}$  in myocytes from failing hearts was more dependent on APD than in controls, particularly at the 6-second cycle length. ANCOVA yielded a coefficient of variation of 0.69 for the failing group compared with 0.18 in controls. By analyzing the late exponentially decaying phase of the  $\text{Ca}^{2+}$  transient (as illustrated in Figure 2A), it was also possible to detect an inherent defect in the time constant for  $\text{Ca}^{2+}$  removal ( $\tau_{\text{Ca}}$ ) in cells from failing hearts (Figure 2C); however, from action potential-stimulated  $\text{Ca}^{2+}$  transients, it is difficult to distinguish inherent changes in  $\text{Ca}^{2+}$  regulatory subsystems from altered  $\text{Ca}^{2+}$  kinetics secondary to electrophysiological (ie, action potential waveform) changes. Therefore, the various  $\text{Ca}^{2+}$  removal subsystems were selectively examined with voltage-clamp techniques.

### Voltage-Clamp-Stimulated $\text{Ca}^{2+}$ Transients in Physiological Solutions

Voltage-clamp experiments permitted the direct measurement of the  $\text{Ca}^{2+}$  removal rate at a fixed voltage ( $-97$  mV) after a 200-ms-long depolarizing step (to  $+3$  mV). Figure 3A and 3B shows representative membrane currents and  $\text{Ca}^{2+}$  waveforms for myocytes from control and failing hearts. The membrane current records during the depolarizing step in physiological salt solution reflect overlapping  $\text{Na}^+$  current, L-type  $\text{Ca}^{2+}$  current, transient outward  $\text{K}^+$  current, and transient outward  $\text{Ca}^{2+}$ -activated  $\text{Cl}^-$  current, among others; therefore, we did not directly measure the amplitude of  $I_{\text{Ca}}$  under these conditions (see Figure 4 for comparisons of  $I_{\text{Ca}}$  between groups in  $\text{Na}^+$ -free,  $\text{K}^+$ -free solutions). No significant difference in resting  $\text{Ca}^{2+}$  was evident under these conditions; however, peak systolic  $\text{Ca}^{2+}$  was reduced 40% to 50% in cells from failing hearts (mean data are shown in Figure 7). The time constant for  $\text{Ca}^{2+}$  removal ( $\tau_{\text{Ca}}$ ) was 35% longer in the failing group under physiological conditions (control,  $216 \pm 25$  ms,  $n=17$ ; failing,  $292 \pm 23$  ms,  $n=22$ ;  $P < 0.05$ ; Figure 3E).

### Voltage-Clamp-Stimulated $\text{Ca}^{2+}$ Transients in $\text{Na}^+$ -Free Solutions

The prolongation of  $\tau_{\text{Ca}}$  in the failing group was markedly accentuated when cells were studied in  $\text{Na}^+$ -free,  $\text{K}^+$ -free intracellular and extracellular solutions (Figure 3C through 3E,  $-\text{Na}$  data). Under these conditions,  $\tau_{\text{Ca}}$  almost exclusively represents the SR  $\text{Ca}^{2+}$  uptake rate; mitochondrial and sarcolemmal  $\text{Ca}^{2+}$  removal processes likely contribute  $< 2\%$  to the total  $\text{Ca}^{2+}$  decay rate.<sup>39</sup> In control cells,  $\tau_{\text{Ca}}$  was prolonged by  $\approx 30\%$  in  $\text{Na}^+$ -free solution ( $282 \pm 30$  ms,  $n=13$ ) compared with physiological solutions. In cells from failing hearts,  $\tau_{\text{Ca}}$  was prolonged by 97% ( $576 \pm 83$  ms,  $n=11$ ) relative to that in physiological solutions and was twice as slow as in the control group ( $P < 0.005$ ). Since  $\text{Na}^+$ -free conditions effectively eliminate  $\text{Na}^+/\text{Ca}^{2+}$  exchange, the results indicate that myocytes from failing hearts have a greater reliance on  $\text{Na}^+/\text{Ca}^{2+}$  exchange for removing  $\text{Ca}^{2+}$  from the cytoplasm during a transient. The  $\tau_{\text{Ca}}$  in  $\text{Na}^+$ -free solution is

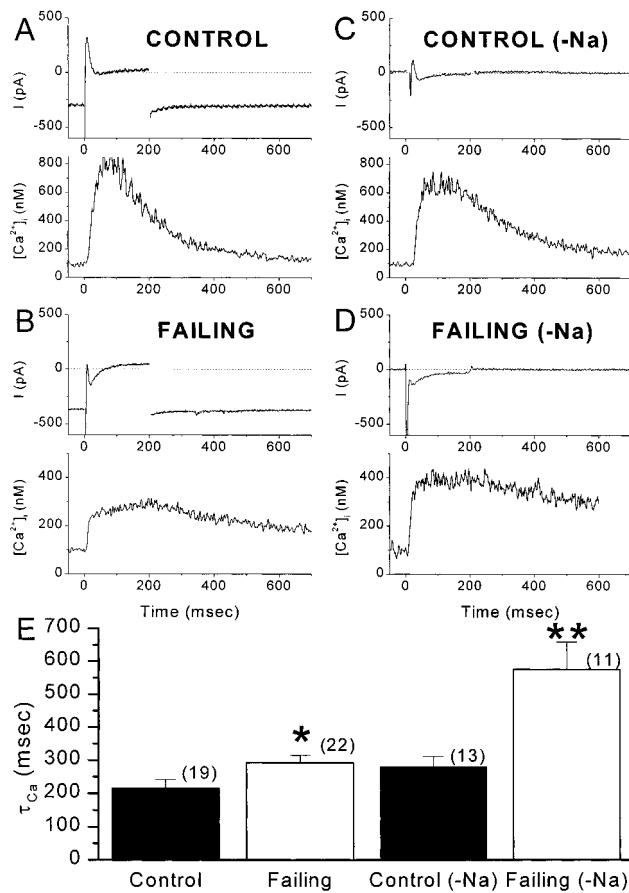


**Figure 3.** Comparison of Ca<sup>2+</sup> removal rates in the presence and absence of Na<sup>+</sup>/Ca<sup>2+</sup> exchange. A, Top panel, membrane current record during a 200-ms voltage-clamp step from a holding potential of -97 mV to +3 mV (initiated at time 0) in a control myocyte in physiological solution. Bottom panel, Ca<sup>2+</sup> transient evoked by the voltage-clamp step described above. B, Membrane current record (top panel) and Ca<sup>2+</sup> transient (bottom panel) for a similar voltage-clamp step in a myocyte from a failing heart. C, Membrane current record (top panel) and Ca<sup>2+</sup> transient (bottom panel) for a control myocyte in the absence of Na<sup>+</sup>/Ca<sup>2+</sup> exchange (-Na). Ca<sup>2+</sup> and Cl<sup>-</sup> were the only permeant ions present in the internal and external solutions. D, Membrane current record (top panel) and Ca<sup>2+</sup> transient (bottom panel) in a myocyte from a failing heart under the same conditions as in panel C. E, The time constants for Ca<sup>2+</sup> removal (τ<sub>Ca</sub>) in the presence and absence (-Na) of Na<sup>+</sup>/Ca<sup>2+</sup> exchange. Ca<sup>2+</sup> removal was prolonged more by eliminating Na<sup>+</sup>/Ca<sup>2+</sup> exchange in cells from failing hearts compared with controls. Values are mean ± SE for the number of myocytes indicated above each bar from 9 control hearts and 6 failing hearts for data in physiological solutions; -Na data are from 4 control hearts and 3 failing hearts. \**P* < 0.05; \*\**P* < 0.005.

a direct measure of the primary defect in Ca<sup>2+</sup> removal in heart failure—suppressed SR Ca<sup>2+</sup> uptake.

The alterations in Ca<sup>2+</sup> handling were not due to differences in the amplitude of the trigger for Ca<sup>2+</sup> release nor to a change in the voltage dependence of the evoked Ca<sup>2+</sup> transient. In Na<sup>+</sup>-free, K<sup>+</sup>-free solutions, there was no difference in the voltage dependence or density of I<sub>Ca</sub> between groups (Figure 4A and 4B). Similarly, the midpoint of activation of the Ca<sup>2+</sup> transient and the position of the maximum of the Ca<sup>2+</sup> transient—versus-voltage curve were not altered by heart failure (Figure 4C and 4D). At potentials more positive than the peak of this curve, the

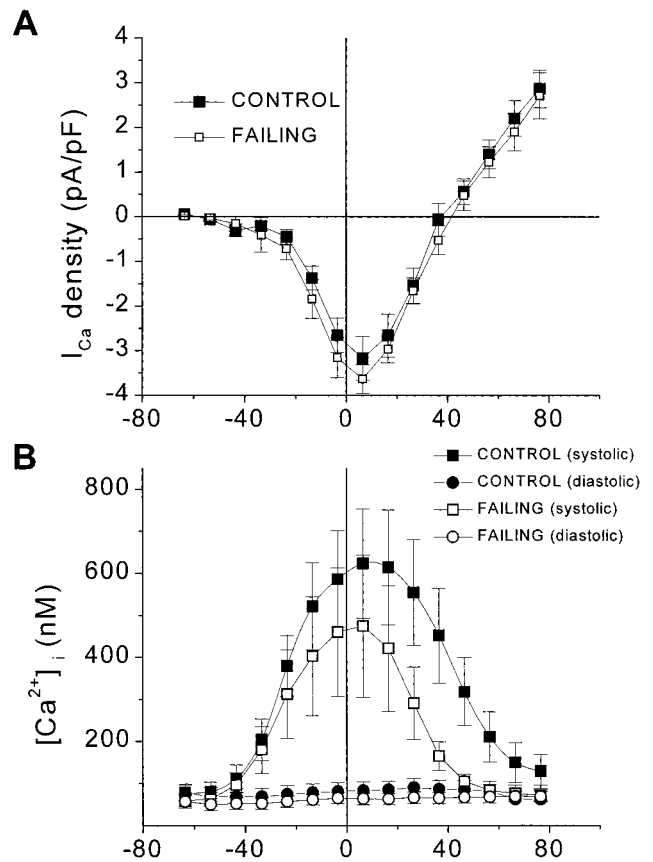


**Figure 4.** Voltage dependence of Ca<sup>2+</sup> currents and Ca<sup>2+</sup> transients in cardiomyocytes from control and failing hearts. A, Peak inward Ca<sup>2+</sup> current density during a 200-ms voltage-clamp step from a holding potential of -97 mV to +3 mV (initiated at time 0) in a control myocyte in physiological solution. Bottom panel, Ca<sup>2+</sup> transient evoked by the voltage-clamp step described above. B, Membrane current record (top panel) and Ca<sup>2+</sup> transient (bottom panel) for a similar voltage-clamp step in a myocyte from a failing heart. C, Membrane current record (top panel) and Ca<sup>2+</sup> transient (bottom panel) for a control myocyte in the absence of Na<sup>+</sup>/Ca<sup>2+</sup> exchange (-Na). Ca<sup>2+</sup> and Cl<sup>-</sup> were the only permeant ions present in the internal and external solutions. D, Membrane current record (top panel) and Ca<sup>2+</sup> transient (bottom panel) in a myocyte from a failing heart under the same conditions as in panel C. E, The time constants for Ca<sup>2+</sup> removal (τ<sub>Ca</sub>) in the presence and absence (-Na) of Na<sup>+</sup>/Ca<sup>2+</sup> exchange. Ca<sup>2+</sup> removal was prolonged more by eliminating Na<sup>+</sup>/Ca<sup>2+</sup> exchange in cells from failing hearts compared with controls. Values are mean ± SE for the number of myocytes indicated above each bar from 9 control hearts and 6 failing hearts for data in physiological solutions; -Na data are from 4 control hearts and 3 failing hearts. \**P* < 0.05; \*\**P* < 0.005.

voltage dependence of the Ca<sup>2+</sup> transient appeared elevated with respect to the failing group (NS).

### Effect of Ca<sup>2+</sup> ATPase Inhibition

A second test of the hypothesis that Na<sup>+</sup>/Ca<sup>2+</sup> exchange accounts for a greater fraction of Ca<sup>2+</sup> removal in cells from failing hearts was to determine the rate of Ca<sup>2+</sup> removal with SR uptake blocked. The SR Ca<sup>2+</sup> ATPase inhibitor CPA (100 μmol/L) reduced the amplitude of the Ca<sup>2+</sup> transient and greatly prolonged Ca<sup>2+</sup> removal in both experimental groups (Figure 5A). This effect was larger in the control group, and the final τ<sub>Ca</sub> in CPA was 46% slower in the control group than in the failing group (Figure 5B). In the presence of CPA, τ<sub>Ca</sub> increased by 236 ± 42% (n = 9) in myocytes from control hearts as compared with an increase of only 102 ± 31% (n = 8; *P* < 0.05) in the failing group (Figure 5C). The results indicate that during a physiological Ca<sup>2+</sup> transient, a greater fraction of Ca<sup>2+</sup> removal is contributed by Na<sup>+</sup>/Ca<sup>2+</sup> exchange than by SR Ca<sup>2+</sup> uptake in failing myocytes.

### Effect of β-Adrenergic Stimulation

There is evidence that β-adrenergic receptors are decreased in heart failure<sup>7-13</sup>; thus it was of interest to determine the extent

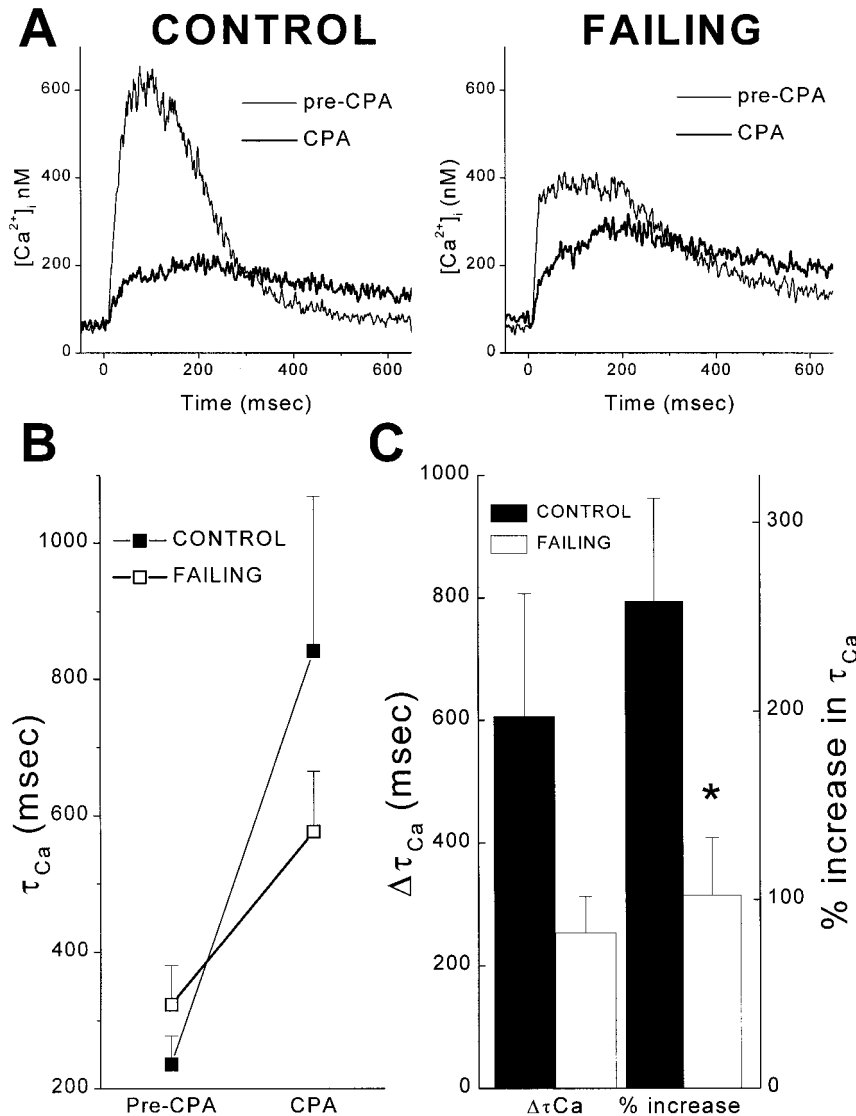


**Figure 5.** Effect of SERCA2a inhibition on cytosolic  $Ca^{2+}$  transients. A,  $Ca^{2+}$  transients were evoked by voltage-clamp steps such as those in Figure 3A and 3B in myocytes from control (left) and failing (right) hearts in physiological solutions (6-second cycle length). B,  $\tau_{Ca}$  before (pre-CPA) and after (CPA) application of CPA (100  $\mu$ mol/L). Exponential fits were made to the falling phase of the transients beginning  $\approx$ 20 ms after repolarization to the holding potential ( $-97$  mV). C, Change ( $\Delta\tau_{Ca}$ ; left) and percentage increase (right) in  $\tau_{Ca}$  illustrates the greater reliance on  $Na^+/Ca^{2+}$  exchange in myocytes from failing hearts. Data shown are mean  $\pm$  SE. \* $P < 0.05$ .

to which the limitations of SR  $Ca^{2+}$  handling could be reversed by inotropic intervention. With  $Na^+/Ca^{2+}$  exchange blocked using Na-free solutions, the ability to upregulate SR  $Ca^{2+}$  uptake by  $\beta$ -adrenergic stimulation was assessed by treatment with isoproterenol (ISO; 1  $\mu$ mol/L). ISO accelerated  $\tau_{Ca}$  in both experimental groups (Figure 6A); however, the absolute  $\tau_{Ca}$  remained significantly longer in the failing group under  $\beta$ -adrenergic stimulation and fell within the range of unstimulated controls (control  $\tau_{Ca}$ ,  $66 \pm 4$  ms,  $n=7$ ; failing  $\tau_{Ca}$ ,  $207 \pm 65$  ms,  $n=7$ ;  $P < 0.05$ ). The change in  $\tau_{Ca}$  ( $\Delta\tau_{Ca}$ ) was significantly greater in myocytes from failing hearts (Figure 6C), perhaps owing to the slow initial rate, but the percentage decrease in  $\tau_{Ca}$  was similar in both groups ( $\approx 70\%$ ; Figure 6C).

### Effect of Frequency on $Ca^{2+}$ Transients

A significant shift toward transsarcolemmal  $Ca^{2+}$  extrusion coupled with downregulation of SR  $Ca^{2+}$  uptake would be expected to result in decreased loading of the SR at faster pacing frequencies. In this regard, suppressed frequency-dependent enhancement of contraction has been demon-

strated in human heart failure.<sup>18,20,32,40</sup> In physiological solutions under voltage-clamp conditions, control myocytes had higher peak systolic  $Ca^{2+}$  levels over a wide range of frequencies compared with cells from failing hearts, and the frequency-dependent enhancement of  $Ca^{2+}$  transient amplitude evident in controls at the 1-second cycle length was absent in the failing group (Figure 7).

### $Ca^{2+}$ Regulatory Protein Expression in Heart Failure

Western blots were used to determine whether the physiological changes in  $Ca^{2+}$  handling with heart failure were correlated with altered protein levels of SERCA2, PLB, and NCX. As is clearly evident in the representative western blots shown in Figure 8A, the pattern of altered protein expression in failing hearts was in line with the idea that SERCA2 is downregulated in heart failure. Both SERCA2 and PLB were reduced by  $\approx 28\%$  in failing hearts (Figure 8B), with no change in the ratio of SERCA2 to PLB. NCX levels were increased by 104% in failing hearts relative to controls (Figure 8B).

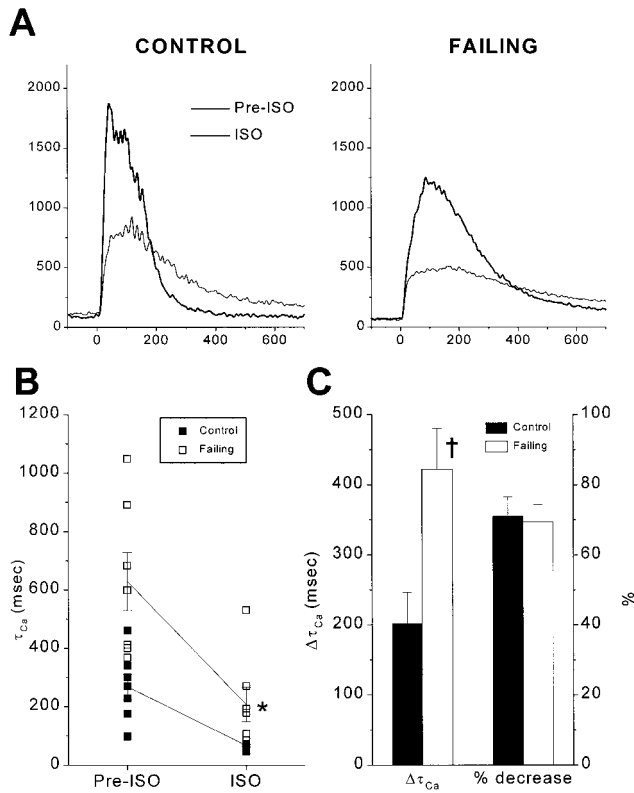


**Figure 6.** Effects of  $\beta$ -adrenergic stimulation of SR  $Ca^{2+}$  uptake. A, Acceleration of SR  $Ca^{2+}$  uptake with  $\beta$ -adrenergic stimulation ( $1 \mu\text{mol/L}$  ISO) in myocytes from control (left) and failing (right) hearts.  $Ca^{2+}$  transients were elicited by voltage-clamp steps in  $Na^+$ -free,  $K^+$ -free solutions at a 6-second cycle length. B,  $\tau_{Ca}$  values from individual myocytes before (pre-ISO) and after (ISO)  $\beta$ -adrenergic stimulation. Lines connect means and SE bars of the data sets. \* $P < 0.05$  for comparison of  $\tau_{Ca}$  in control and failing groups in the presence of ISO. C,  $\beta$ -Adrenergic stimulation decreased  $\tau_{Ca}$  by  $\approx 70\%$  in both experimental groups (right), but the absolute change in  $\tau_{Ca}$  ( $\Delta\tau_{Ca}$ ; left) was significantly larger in the failing group ( $\dagger P < 0.01$ ). Data were obtained under  $Na^+$ -free conditions for  $n = 7$  myocytes from 3 hearts in each group.

### Discussion

Mechanistic studies of human heart failure are complicated by the prolonged time course of development of the disease, the technical challenges of isolating cardiac tissue or cells

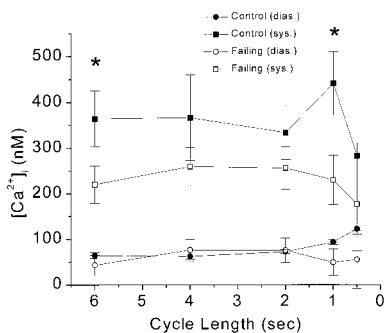


**Figure 7.** Frequency dependence of the  $Ca^{2+}$  transient. Peak systolic  $Ca^{2+}$  was higher in myocytes from control hearts over a range of cycle lengths compared with those in the failing group. Enhancement of the transient at the 1-second interval was absent in cells from failing hearts.  $Ca^{2+}$  transients were elicited by voltage-clamp steps in physiological solutions as in Figure 3A and 3B. \* $P < 0.05$ . Data are mean  $\pm$  SE.

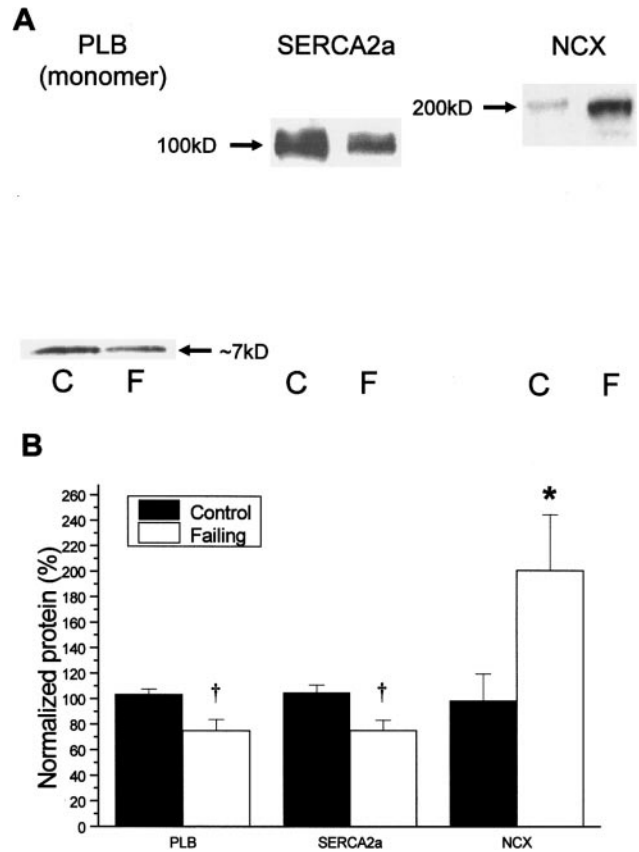


**Figure 8.** Levels of proteins involved in  $Ca^{2+}$  homeostasis in control and failing hearts. A, Western blots showing typical band densities of PLB, SERCA2, and NCX in control and failing hearts (C indicates control, and F, failing). Arrows indicate positions of molecular weight markers run concomitantly. B, Levels of PLB, SERCA2a, and NCX normalized to a reference sample as described in Materials and Methods. Data are from 8 control hearts and 8 failing hearts. \* $P < 0.05$ ;  $\dagger P < 0.01$ .

from explanted hearts, the inability to investigate the early time course of cellular alterations, and the lack of control over experimental conditions. Thus, it is fortunate that the canine tachycardia-induced heart failure model so closely reproduces the known hemodynamic and ionic changes that have been identified in human hearts. The present findings indicate that, in addition to the electrophysiological changes noted in earlier studies, significant alterations in  $Ca^{2+}$  handling occur in isolated myocytes from failing hearts, following the general pattern of human studies. Through biochemical and functional measurements in the same hearts, we have found strong evidence in support of the hypothesis that the induction of heart failure triggers a shift in the balance of cytosolic  $Ca^{2+}$  extrusion mechanisms from SR  $Ca^{2+}$  uptake toward transsarcolemmal  $Ca^{2+}$  removal.

The decrease in peak systolic  $Ca^{2+}$  and prolongation of  $\tau_{Ca}$  are in good agreement with data obtained from human myocytes isolated from terminally failing hearts<sup>2,24</sup>; however, we observed no statistically significant increase in resting  $Ca^{2+}$ . The latter may be explained if  $Na^+/Ca^{2+}$  exchange fully compensates for the reduction of SR  $Ca^{2+}$  uptake in this experimental model. Recent evidence suggests that in human heart failure, the extent of diastolic dysfunction was inversely

correlated with upregulation of  $\text{Na}^+/\text{Ca}^{2+}$  exchange protein.<sup>41</sup> Our observations that the level of NCX protein was approximately double that of control hearts, and the lack of a rise in resting  $\text{Ca}^{2+}$ , indicate that  $\text{Na}^+/\text{Ca}^{2+}$  exchange effectively compensates for defective SR  $\text{Ca}^{2+}$  removal from the cytoplasm. Although there was strong evidence that the fractional contribution of  $\text{Na}^+/\text{Ca}^{2+}$  exchange to  $\text{Ca}^{2+}$  removal during a transient was increased in myocytes from failing cells, the relatively small increase in  $\tau_{\text{Ca}}$  (46%) in the presence of CPA indicates that the function of the NCX may not be increased as much as the protein levels would indicate. This is borne out by the results of the modeling studies, in which only a 53% to 75% functional enhancement of  $\text{Na}^+/\text{Ca}^{2+}$  exchange was estimated by constraining the SR  $\text{Ca}^{2+}$  uptake rate to the value determined experimentally in Na-free conditions.<sup>35</sup> The extent of functional enhancement of  $\text{Na}^+/\text{Ca}^{2+}$  exchange activity in the failing heart will require further investigation, including direct measurements of  $\text{Na}^+/\text{Ca}^{2+}$  exchange current; however, even without an increase in the absolute density of  $\text{Na}^+/\text{Ca}^{2+}$  exchange, a substantially larger  $\text{Na}^+/\text{Ca}^{2+}$  exchange current will be generated during an action potential-evoked  $\text{Ca}^{2+}$  transient in a failing myocyte, as a result of the reduction in SR  $\text{Ca}^{2+}$  uptake. Conversely, the  $\approx 30\%$  decrease in SERCA2 protein levels is likely to be an underestimation of the functional impairment of SR  $\text{Ca}^{2+}$  uptake, which was 2-fold slower in myocytes from failing hearts (see Figure 3E, -Na bars, and Reference 35).

Impaired SR loading from the combined effect of reduced SR  $\text{Ca}^{2+}$  ATPase activity and enhanced transsarcolemmal extrusion could underlie the observed reduction in peak  $\text{Ca}^{2+}$  and frequency-dependent facilitation of  $\text{Ca}^{2+}$  transient amplitude. In this regard, in a parallel study, we have examined the effects of reducing SR  $\text{Ca}^{2+}$  ATPase and increasing  $\text{Na}^+/\text{Ca}^{2+}$  exchange by the amounts determined experimentally in a computer model of the normal and failing canine cardiac cell.<sup>35</sup> The effects on the  $\text{Ca}^{2+}$  transient were well reproduced in the model simulations, indicating that these alterations alone are sufficient to account for the data. We have not directly addressed alternative explanations for the failure-induced alterations in  $\text{Ca}^{2+}$  handling, which include impaired responsiveness of SR  $\text{Ca}^{2+}$  release channels,<sup>42,43</sup> reduced L-type  $\text{Ca}^{2+}$  channel-to-SR  $\text{Ca}^{2+}$  release channel coupling,<sup>44</sup> or loss of frequency-dependent  $\text{Ca}^{2+}$  current facilitation,<sup>45</sup> instead focusing primarily on  $\text{Ca}^{2+}$ -removal mechanisms. As in our previous study,<sup>1</sup> we observed no significant difference in peak L-type  $\text{Ca}^{2+}$  current density in myocytes from failing hearts when compared with controls; however, in light of the alterations in  $\text{Ca}^{2+}$  handling, we would expect that during a given action potential, differences in sarcolemmal subspace  $\text{Ca}^{2+}$  in heart failure would significantly influence  $\text{Ca}^{2+}$ -dependent fast inactivation of L-type  $\text{Ca}^{2+}$  channels. The possible contribution of this effect to action potential prolongation is explored in Winslow et al.<sup>35</sup>

The 28% reduction of SERCA2 protein level is close to that reported by Hasenfuss et al<sup>18</sup> for failing human heart. Unlike in earlier studies, however, PLB levels were reduced by a similar amount, and the ratio of SERCA2 to PLB was not changed. Thus, the functional deficit of SR  $\text{Ca}^{2+}$  uptake could not be explained by a disproportionately higher amount of

PLB but still could involve a difference in the basal phosphorylation state of this protein. Even when phosphorylation was substantially increased by  $\beta$ -adrenergic stimulation, the SR  $\text{Ca}^{2+}$  uptake rate in myocytes from failing hearts was brought only to the level of unstimulated controls, implying a fundamental limitation to the extent of inotropic reserve through the  $\beta$ -adrenergic pathway.

Enhanced  $\text{Na}^+/\text{Ca}^{2+}$  exchange activity during the  $\text{Ca}^{2+}$  transient (whether relative or absolute) may prove to be a pivotal mechanistic change occurring in heart failure. The clear beneficial effect of this  $\text{Ca}^{2+}$  removal mechanism is that it largely compensates for defective SR  $\text{Ca}^{2+}$  uptake. It has also been suggested that enhanced reverse-mode ( $\text{Ca}^{2+}$  entry) activity of the exchanger may provide inotropic support in the failing muscle.<sup>32</sup> On the other hand, forward-mode  $\text{Na}^+/\text{Ca}^{2+}$  exchange in the face of slowed SR  $\text{Ca}^{2+}$  uptake depletes the releasable pool of  $\text{Ca}^{2+}$  with repetitive stimulation, which would effectively unload the SR and alter the frequency-dependent response.<sup>39</sup> Furthermore, since the exchanger is electrogenic, it is likely to participate both directly and indirectly (by influencing SR  $\text{Ca}^{2+}$  load) in reshaping the action potential in the failing heart. In this regard, the most striking finding of the experimental and modeling studies is that alterations in  $\text{Ca}^{2+}$  handling can have major effects on the action potential waveform. In model simulations of minimally  $\text{Ca}^{2+}$ -buffered cardiomyocytes, decreasing the density of  $\text{K}^+$  currents has less effect on the duration of the action potential than does suppression of SR  $\text{Ca}^{2+}$  uptake with enhanced  $\text{Na}^+/\text{Ca}^{2+}$  exchange.<sup>35</sup> The latter effect may predispose failing heart cells to instabilities of repolarization such as early or delayed afterdepolarizations<sup>46</sup> or to triggered activity, especially in  $\text{Ca}^{2+}$ -overloaded myocytes.

In summary, canine pacing-induced heart failure leads to alterations of both the electrophysiological and the  $\text{Ca}^{2+}$  handling properties of cardiomyocytes that are remarkably similar to those described for the human disease. The increased dependence on  $\text{Na}^+/\text{Ca}^{2+}$  exchange coupled with a reduction of SR  $\text{Ca}^{2+}$  uptake not only substantially alters the kinetics and amplitude of the  $\text{Ca}^{2+}$  transient, but is likely to contribute to the altered action potential waveform of the failing heart cell. Continued investigation into the interplay between  $\text{Ca}^{2+}$  handling and membrane potential will be crucial to understanding the pathophysiology of heart failure.

### Acknowledgment

This work was supported by the Specialized Center of Research on Sudden Cardiac Death (NIH P50 HL52307) and R01HL61711.

### References

1. Kääh S, Nuss HB, Chiamvimonvat N, O'Rourke B, Pak PH, Kass DA, Marban E, Tomaselli GF. Ionic mechanism of action potential prolongation in ventricular myocytes from dogs with pacing-induced heart failure. *Circ Res.* 1996;78:262-273.
2. Beuckelmann DJ, Nabauer M, Erdmann E. Intracellular calcium handling in isolated ventricular myocytes from patients with terminal heart failure. *Circulation.* 1992;85:1046-1055.
3. Li HG, Jones DL, Yee R, Klein GJ. Electrophysiologic substrate associated with pacing-induced heart failure in dogs: potential value of programmed stimulation in predicting sudden death. *J Am Coll Cardiol.* 1992;19:444-449.

4. Vermeulen JT, McGuire MA, Ophof T, Coronel R, de BJM, Klopping C, Janse MJ. Triggered activity and automaticity in ventricular trabeculae of failing human and rabbit hearts. *Cardiovasc Res.* 1994;28:1547–1554.
5. Beuckelmann DJ, Nabauer M, Erdmann E. Alterations of  $K^+$  currents in isolated human ventricular myocytes from patients with terminal heart failure. *Circ Res.* 1993;73:379–385.
6. Nabauer M, Beuckelmann DJ, Erdmann E. Characteristics of transient outward current in human ventricular myocytes from patients with terminal heart failure. *Circ Res.* 1993;73:386–394.
7. Li HG, Jones DL, Yee R, Klein GJ. Arrhythmogenic effects of catecholamines are decreased in heart failure induced by rapid pacing in dogs. *Am J Physiol.* 1993;265(part 2):H1654–H1662.
8. Koumi S, Backer CL, Arentzen CE, Sato R.  $\beta$ -Adrenergic modulation of the inwardly rectifying potassium channel in isolated human ventricular myocytes. alteration in channel response to  $\beta$ -adrenergic stimulation in failing human hearts. *J Clin Invest.* 1995;96:2870–2881.
9. Newman WH. Volume overload heart failure: length-tension curves, and response to  $\beta$ -agonists,  $Ca^{2+}$ , and glucagon. *Am J Physiol.* 1978;235:H690–H700.
10. Fowler MB, Laser JA, Hopkins GL, Minobe W, Bristow MR. Assessment of the  $\beta$ -adrenergic receptor pathway in the intact failing human heart: progressive receptor down-regulation and subsensitivity to agonist response. *Circulation.* 1986;74:1290–1302.
11. Feldman MD, Copelas L, Gwathmey JK, Phillips P, Warren SE, Schoen FJ, Grossman W, Morgan JP. Deficient production of cyclic AMP: pharmacologic evidence of an important cause of contractile dysfunction in patients with end-stage heart failure. *Circulation.* 1987;75:331–339.
12. Bohm M, Beuckelmann D, Brown L, Feiler G, Lorenz B, Nabauer M, Kemkes B, Erdmann E. Reduction of  $\beta$ -adrenoceptor density and evaluation of positive inotropic responses in isolated, diseased human myocardium. *Eur Heart J.* 1988;9:844–852.
13. Nabauer M, Bohm M, Brown L, Diet F, Eichhorn M, Kemkes B, Pieske B, Erdmann E. Positive inotropic effects in isolated ventricular myocardium from non-failing and terminally failing human hearts. *Eur J Clin Invest.* 1988;18:600–606.
14. Morgan JP. Intracellular calcium in heart failure. *Cardiovasc Drugs Ther.* 1988;1:621–624.
15. Gwathmey JK, Copelas L, MacKinnon R, Schoen FJ, Feldman MD, Grossman W, Morgan JP. Abnormal intracellular calcium handling in myocardium from patients with end-stage heart failure. *Circ Res.* 1987;61:70–76.
16. Meuse AJ, Perreault CL, Morgan JP. Pathophysiology of cardiac hypertrophy and failure of human working myocardium: abnormalities in calcium handling. *Basic Res Cardiol.* 1992;87(suppl 1):223–233.
17. Perreault CL, Shannon RP, Komamura K, Vatner SF, Morgan JP. Abnormalities in intracellular calcium regulation and contractile function in myocardium from dogs with pacing-induced heart failure. *J Clin Invest.* 1992;89:932–938.
18. Hasenfuss G, Reinecke H, Studer R, Pieske B, Meyer M, Drexler H, Just H. Calcium cycling proteins and force-frequency relationship in heart failure. *Basic Res Cardiol.* 1996;91(suppl 2):17–22.
19. Pieske B, Hasenfuss G, Holubarsch C, Schwinger R, Bohm M, Just H. Alterations of the force-frequency relationship in the failing human heart depend on the underlying cardiac disease. *Basic Res Cardiol.* 1992;87(suppl 1):213–221.
20. Phillips PJ, Gwathmey JK, Feldman MD, Schoen FJ, Grossman W, Morgan JP. Post-extrasystolic potentiation and the force-frequency relationship: differential augmentation of myocardial contractility in working myocardium from patients with end-stage heart failure. *J Mol Cell Cardiol.* 1990;22:99–110.
21. del Monte F, O'Gara P, Poole-Wilson PA, Yacoub M, Harding SE. Cell geometry and contractile abnormalities of myocytes from failing human left ventricle. *Cardiovasc Res.* 1995;30:281–290.
22. Davies CH, Davia K, Bennett JG, Pepper JR, Poole-Wilson PA, Harding SE. Reduced contraction and altered frequency response of isolated ventricular myocytes from patients with heart failure. *Circulation.* 1995;92:2540–2549.
23. Beuckelmann DJ, Erdmann E.  $Ca(2+)$ -currents and intracellular  $[Ca^{2+}]_i$ -transients in single ventricular myocytes isolated from terminally failing human myocardium. *Basic Res Cardiol.* 1992;87(suppl 1):235–243.
24. Beuckelmann DJ, Nabauer M, Kruger C, Erdmann E. Altered diastolic  $[Ca^{2+}]_i$  handling in human ventricular myocytes from patients with terminal heart failure. *Am Heart J.* 1995;129:684–689.
25. Hasenfuss G, Meyer M, Schillinger W, Preuss M, Pieske B, Just H. Calcium handling proteins in the failing human heart. *Basic Res Cardiol.* 1997;92(suppl 1):87–93.
26. Arai M, Alpert NR, MacLennan DH, Barton P, Periasamy M. Alterations in sarcoplasmic reticulum gene expression in human heart failure: a possible mechanism for alterations in systolic and diastolic properties of the failing myocardium. *Circ Res.* 1993;72:463–469.
27. Flesch M, Schwinger RH, Schnabel P, Schiffer F, van Gelder I, Bavendiek U, Sudkamp M, Kuhn-Regnier F, Bohm M. Sarcoplasmic reticulum  $Ca^{2+}$  ATPase and phospholamban mRNA and protein levels in end-stage heart failure due to ischemic or dilated cardiomyopathy. *J Mol Med.* 1996;74:321–332.
28. Movsesian MA, Karimi M, Green K, Jones LR.  $Ca^{2+}$ -transporting ATPase, phospholamban, and calsequestrin levels in nonfailing and failing human myocardium. *Circulation.* 1994;90:653–657.
29. Schwinger RH, Bohm M, Schmidt U, Karczewski P, Bavendiek U, Flesch M, Krause EG, Erdmann E. Unchanged protein levels of SERCA II and phospholamban but reduced  $Ca^{2+}$  uptake and  $Ca^{2+}$ -ATPase activity of cardiac sarcoplasmic reticulum from dilated cardiomyopathy patients compared with patients with nonfailing hearts. *Circulation.* 1995;92:3220–3228.
30. Movsesian MA, Bristow MR, Krall J.  $Ca^{2+}$  uptake by cardiac sarcoplasmic reticulum from patients with idiopathic dilated cardiomyopathy. *Circ Res.* 1989;65:1141–1144.
31. Studer R, Reinecke H, Bilger J, Eschenhagen T, Bohm M, Hasenfuss G, Just H, Holtz J, Drexler H. Gene expression of the cardiac  $Na^+-Ca^{2+}$  exchanger in end-stage human heart failure. *Circ Res.* 1994;75:443–453.
32. Flesch M, Schwinger RH, Schiffer F, Frank K, Sudkamp M, Kuhn-Regnier F, Arnold G, Bohm M. Evidence for functional relevance of an enhanced expression of the  $Na^+-Ca^{2+}$  exchanger in failing human myocardium. *Circulation.* 1996;94:992–1002.
33. Reinecke H, Studer R, Vetter R, Just H, Holtz J, Drexler H. Role of the cardiac sarcolemmal  $Na^+-Ca^{2+}$  exchanger in end-stage human heart failure. *Ann N Y Acad Sci.* 1996;779:543–545.
34. Reinecke H, Studer R, Vetter R, Holtz J, Drexler H. Cardiac  $Na^+/Ca^{2+}$  exchange activity in patients with end-stage heart failure. *Cardiovasc Res.* 1996;31:48–54.
35. Winslow RL, Rice J, Jafri S, Marbán E, O'Rourke B. Mechanisms of altered excitation-contraction coupling in canine tachycardia-induced heart failure, II: model studies. *Circ Res.* 1999;84:571–586.
36. Neher E. Correction for liquid junction potentials in patch clamp experiments. *Methods Enzymol.* 1992;207:123–131.
37. Grynkiewicz G, Peonie M, Tsien RY. A new generation of  $Ca^{2+}$  indicators with greatly improved fluorescence properties. *J Biol Chem.* 1985;260:3440–3450.
38. Bassani JW, Bassani RA, Bers DM. Calibration of indo-1 and resting intracellular  $[Ca]_i$  in intact rabbit cardiac myocytes. *Biophys J.* 1995;68:1453–1460.
39. Bers DM. *Excitation-Contraction Coupling and Cardiac Contractile Force.* Dordrecht, the Netherlands: Kluwer Academic Publishing; 1991.
40. Hasenfuss G, Holubarsch C, Hermann HP, Astheimer K, Pieske B, Just H. Influence of the force-frequency relationship on haemodynamics and left ventricular function in patients with non-failing hearts and in patients with dilated cardiomyopathy. *Eur Heart J.* 1994;15:164–170.
41. Hasenfuss G, Preuss M, Lehnart S, Prestle J, Meyer M, Just H. Relationship between diastolic function and protein levels of sodium-calcium exchanger in end-stage failing human hearts. *Circulation.* 1996;94(suppl 1):I-433.
42. D'Agnolo A, Luciani GB, Mazzucco A, Gallucci V, Salvati G. Contractile properties and  $Ca^{2+}$  release activity of the sarcoplasmic reticulum in dilated cardiomyopathy. *Circulation.* 1992;85:518–525.
43. Nimer LR, Needleman DH, Hamilton SL, Krall J, Movsesian MA. Effect of ryanodine on sarcoplasmic reticulum  $Ca^{2+}$  accumulation in nonfailing and failing human myocardium. *Circulation.* 1995;92:2504–2510.
44. Gomez AM, Valdivia HH, Cheng H, Lederer MR, Santana LF, Cannell MB, McCune SA, Altschuld RA, Lederer WJ. Defective excitation-contraction coupling in experimental cardiac hypertrophy and heart failure. *Science.* 1997;276:800–806.
45. Piot C, Lemaire S, Albat B, Seguin J, Nargeot J, Richard S. High frequency-induced upregulation of human cardiac calcium currents. *Circulation.* 1996;93:120–128.
46. Fozzard HA. Afterdepolarizations and triggered activity. *Basic Res Cardiol.* 1992;87(suppl 2):105–113.